ESA UNCLASSIFIED – For Official Use

DOCUMENT

RA0598
Proton Irradiation Test Results on Micropac Part Types 66191-313 and 66226-001

Prepared by	**Alessandra Costantino**
Issue	**1**
Revision	**1**
Date of Issue	**30/05/2012**
Status	**Authorized**
Document Type	**Test Report**
Distribution	**External**

European Space Agency
Agence spatiale européenne

APPROVAL

Title Proton Irradiation Test Results on Micropac Part Types 66191-313 and 66226-001	
Issue 1	**Revision** 1
Author Alessandra Costantino	**Date 30/05/2012**
Reviewed by Véronique Ferlet-Cavrois	**Date**
Approved by Stephan Hernandez	**Date**
Authorized by Ali Zadeh	**Date**

CHANGE LOG

Reason for change	Issue	Revision	Date
Added Par.5 :"CTR degradation as function of Displacement Damage Dose"	1	1	30/05/2012

CHANGE RECORD

Issue 1	Revision 1		
Reason for change	**Date**	**Pages**	**Paragraph(s)**
Analysis of CTR degradation as function of Displacement Damage Dose	30/05/2012	27-29	5

Table of contents:

1 INTRODUCTION

1.1 Background

Micropac optocouplers that employ a 2N2222 transistor as amplifier stage are subjected to a transistor die change: the former transistor used, produced by Microsemi, is being replaced by a Micropac in-house produced transistor.
A TID radiation test performed at ESTEC on both old and new versions of reference 66191 (66191-303 and 66191-313) revealed that the 66191-313 devices are more sensitive to low dose rate TID irradiation than 66191-303. The TID test report (RA0585) can be found on the ESA Internal Problem Notification website (ref. IPN #242) and in the Radiation Database on ESCIES website.
Other Micropac references with similar configuration are now using the NPN Micropac transistor: 66191, 66189, 66223, 66225, 66226, 66179, 66099/300. The updated list of devices can be retrieved on IPN#242.

This proton irradiation test was performed to assess the damage caused by radiation on samples from references 66191-313 and 66226-001 employing the Micropac in-house manufactured transistor.

1.2 Devices under test

The part types under test are 66191–313 and 66226-001. These references have the same electrical layout (Fig. 1) consisting of a LED coupled to a photodiode and a 2N2222 transistor.
Both part types employ a 2N2222 transistor manufactured in-house by Micropac, but have different LEDs with the wavelength of 660 nm for 66191 and 850 nm for 66226.

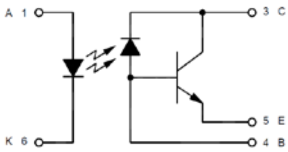

Fig. 1: The electrical layout is the same for both 66191 and 66226 part types.

1.3 Energy and fluence

Proton irradiation was performed on 18th and 19th of January 2012 at AGORFIRM cyclotron in KVI-Groningen.
Three proton energies were selected: 28 MeV, 60 MeV and 184 MeV.
A flux of 2E+8 p/cm^2 was used for the irradiations. Intermediate electrical characterization have been performed at increasing proton fluence levels as reported in Table 1.

fluence steps	Energy		
	28MeV	60MeV	184MeV
1.00E+10	✔		
3.00E+10	✔	✔	✔
7.00E+10	✔	✔	✔
2.00E+11	✔	✔	✔
4.00E+11			✔ (only #24 of 66191-313)
6.00E+11	✔	✔	✔

Table 1: Irradiation history for each board, irradiation flux=2E+8 p/(s*cm^2).

2 IRRADIATION OUTLINE

2.1 Biasing conditions

During the proton irradiation the samples were unbiased with all pins grounded, this was the worst biasing condition that we identified in previous irradiation testing on optocouplers.

2.2 DUT distribution

A summary of the irradiation history is reported in the following tables:

Reference: 66191-313 D/C 1031

Biasing condition	Fluence steps	Energy	DUT S/N	Sample Size
Unbiased: All pins grounded	3.00E+10 7.00E+10 2.00E+11 4.70E+11 (sample#24) 6.00E+11	184MeV	#19, #20, #21, #22, #23, #24, #25, #26, #27	9
	3.00E+10 7.00E+10 2.00E+11 6.00E+11	60 MeV	#10, #11, #12, #13, #15, #16, #17, #18, #28	9
	1.00E+10 3.00E+10 7.00E+10 2.00E+11 6.00E+11	28 MeV	#01, #02, #03, #04, #05, #06, #07, #08, #09	9

Table 2: Summary of the irradiation history for the optocouplers 66191-313 DC1031

Reference: 66226-001 D/C 1112

Biasing condition	Fluence steps	Energy	DUT S/N	Sample Size
Unbiased: All pins grounded	3.00E+10 7.00E+10 2.00E+11 6.00E+11	184MeV	#13, #15, #16, #17, #18, #28	6
	3.00E+10 7.00E+10 2.00E+11 6.00E+11	60 MeV	#07, #08, #09, #10, #11, #12,	6
	1.00E+10 3.00E+10 7.00E+10 2.00E+11 6.00E+11	28 MeV	#01, #02, #03, #04, #05, #06	6

Table 3: Summary of the irradiation history for the optocouplers 66226-001 DC1112

3 ELECTRICAL PARAMETERS TESTED

Electrical measurement reported in Table 4 were performed as initial characterization and after each fluence step (ref. Table 2 and Table 3).
All listed parameters were measured using an Agilent4156C and a text fixture Agilent 16442A. The optocoupler, that have an LCC package, were soldered on 8-pin DIL Winslow adapters.
The measuring sequence was controlled by the Wavewue (Microvue) software.

Tested part	Nr.	Description	Parameter	Units	Limits		Test Condition
					Min	max	
Emitter	1	Input Diode Static Reverse Current	Ir	pA	-	100 nA	Vr=3V
Receiver	2	Collector Base Dark Current	IcbOff	pA		100 uA	Vcb=40V
Receiver	3	Collector Emitter Dark Current	IceOff	pA	-	1 mA	Vce=40V
Receiver	4	Collector Emitter dark current	IceOff	pA	-	100 nA	Vce=20V
OC	5	Collector Emitter Saturation Voltage	Vce_{SAT}	V	-	0.3	If =20mA, Ic=10mA
OC	6	On State Collector Current	Ic	mA	1	-	Vce=1V, If=10mA
OC	7	On State Collector Current - characteristic	Ic	mA	-	-	Vce=1V, If=0.1-40mA

Table 4

The CTR is the parameter generally used to characterize the static efficiency of an optocoupler, it is defined by the ratio of the On State Collector Current (I_C) to the corresponding LED current (I_F).:

$$CTR = \frac{I_C}{I_F}$$

This parameter is included in the results.

4 TEST RESULTS

4.1 Emitter stage

The initial LED reverse current was the parameter tested on the emitter side.
The reverse current of 66191-313 is on average half that of the 66226-001 (respectively 1pA and 2pA).
Fig. 2 illustrate that the 66226-001 is more proton radiation sensitive than the 66191-313: the final reverse current of 66226-001 is approximately two orders of magnitude higher than the 66191-313.

Two DUTs, one for each part type (#04 for 66191 and #07 for 66226), have a high initial reverse current (200pA and 1000pA). In contrast to the other samples these two are not affected by irradiation.
No correlation was found between the high initial leakage current of these two samples with their CTR performances.

4.1.1 Reverse Current drifts

Manufacturer specification: $Ir_{MAX} = 10\ \mu A$.

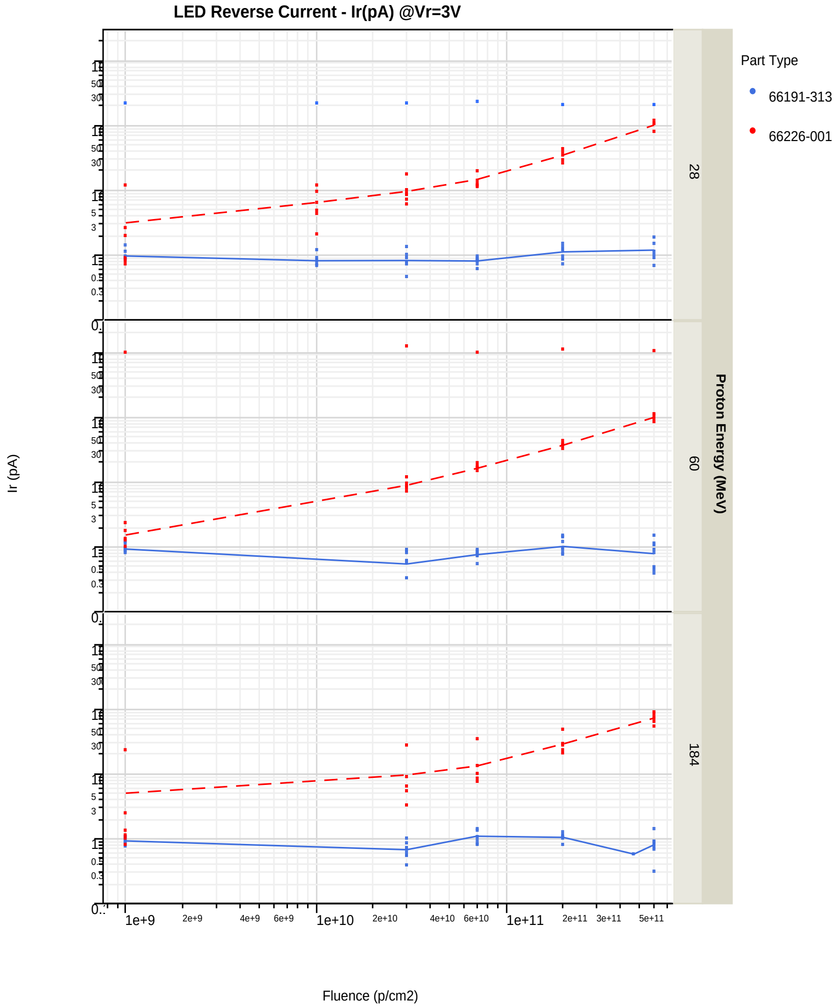

Fig. 2: LED reverse current drift. The points represent the measured data for each sample, and the line shows the trend of the average for each part type.

European Space Agency
Agence spatiale européenne

			Fluence (p/cm2)						
			1e+9	1e+10	3e+10	7e+10	2e+11	4.7e+11	6e+11
			y	y	y	y	y	y	y
Part type	**Proton Energy (MeV)**	**SN**	**Mean**	**Mean**	**Mean**	**Mean**	**Mean**	**Mean**	**Mean**
66191-313	28	#01	-0.83	-0.68	-0.47	-0.81	-1.29	.	-0.87
		#02	-0.86	-1.17	-1.31	-0.59	-1.45	.	-1.83
		#03	-0.92	-0.81	-0.87	-0.87	-0.92	.	-1.08
		#04	-219.55	-212.50	-209.60	-233.10	-205.90	.	-201.40
		#05	-0.88	-0.69	-0.72	-0.95	-1.27	.	-1.11
		#06	-1.38	-0.89	-0.99	-0.90	-1.28	.	-1.47
		#07	-0.84	-0.80	-0.77	-0.73	-1.17	.	-1.49
		#08	-1.11	-0.72	-0.76	-0.84	-0.83	.	-0.67
		#09	-0.91	-0.79	-0.71	-0.78	-0.72	.	-1.00
	60	#10	-0.82	.	-0.89	-0.75	-1.18	.	-0.42
		#11	-0.81	.	-0.56	-0.76	-0.78	.	-1.14
		#12	-0.92	.	-0.77	-0.90	-0.87	.	-0.87
		#13	-1.11	.	-0.59	-0.74	-0.93	.	-0.80
		#15	-0.91	.	-0.84	-0.78	-0.85	.	-0.49
		#16	-0.89	.	-0.32	-0.83	-1.45	.	-1.03
		#17	-1.17	.	-0.55	-0.70	-1.40	.	-1.51
		#18	-0.84	.	-0.32	-0.53	-0.76	.	-0.38
		#28	-0.84	.	0.07	-0.81	-0.92	.	-0.43
	184	#19	-1.02	.	.	-1.34	-1.00	.	-0.83
		#20	-0.96	.	-0.67	-1.04	-1.27	.	-0.72
		#21	-0.75	.	-0.72	-0.78	-0.78	.	-0.78
		#22	-0.83	.	-0.55	-1.41	-0.99	.	-0.91
		#23	-0.97	.	-0.60	-0.97	-1.12	.	-0.68
		#24	-0.82	.	-0.83	-1.31	.	-0.58	.
		#25	-1.03	.	-0.99	-1.35	-1.06	.	-0.88
		#26	-0.87	.	-0.68	-0.79	-1.07	.	-0.30
		#27	-1.06	.	-0.38	-0.84	-1.09	.	-1.36
66226-001	28	#01	-0.73	-4.77	-9.70	-12.53	-37.15	.	-106.50
		#02	-0.87	-6.39	-8.79	-19.48	-42.77	.	-101.40
		#03	-2.59	-4.16	-8.35	-11.45	-33.82	.	-99.62
		#04	-1.91	-9.54	-7.17	-10.91	-25.48	.	-77.49
		#05	-11.94	-11.74	-17.49	-19.26	-41.93	.	-114.90
		#06	-0.79	-2.03	-5.92	-13.83	-28.37	.	-104.90
	60	#07	-991.60	.	-1201.00	-974.10	-1123.00	.	-1046.00
		#08	-2.26	.	-8.22	-16.35	-38.08	.	-105.90
		#09	-1.77	.	-9.58	-19.02	-35.61	.	-90.57
		#10	-0.98	.	-12.03	-17.01	-35.81	.	-110.00
		#11	-1.34	.	-6.99	-14.42	-32.54	.	-82.48
		#12	-1.27	.	-7.70	-14.21	-43.37	.	-107.70
	184	#13	-1.08	.	-6.42	-8.21	-23.18	.	-54.29
		#14	-23.52	.	-27.69	-33.16	-47.91	.	-83.22
		#15	-1.33	.	-8.62	-13.23	-29.13	.	-64.62
		#16	-2.51	.	-6.32	-10.03	-26.28	.	-88.54
		#17	-0.78	.	-5.42	-7.41	-20.66	.	-73.64
		#18	-1.01	.	-3.23	-7.26	-26.84	.	-71.19

Table 5: LED reverse current at increasing fluence for each tested device.

4.2 Receiver stage:

Dark current measurements were performed on the photodiode receiver stage. All initial and intermediate data are compliant with the manufacturer specification except for one sample of part type 66191-313 (#17) which after a fluence of 2E+11 p/cm² has a Collector Emitter Dark Current above the manufacturer maximum rated dark current.
Even if compliant with manufacturer specifications, 6 of the 28 samples tested of part type 66191-313 showed high post irradiation dark current levels. Up to 2 orders of magnitude over the average (eg. IcbOFF@40V is above 1E+5pA, compared to an average of 1E+3pA). A screening could identify these samples, whose dark currents are the most affected by radiation, as their initial dark current is over the double of 66191-313 mean dark currents.
For the 6 samples mentioned above, no correlation was found between the high current leakages and CTR performances.

4.2.1 Collector base dark current drifts

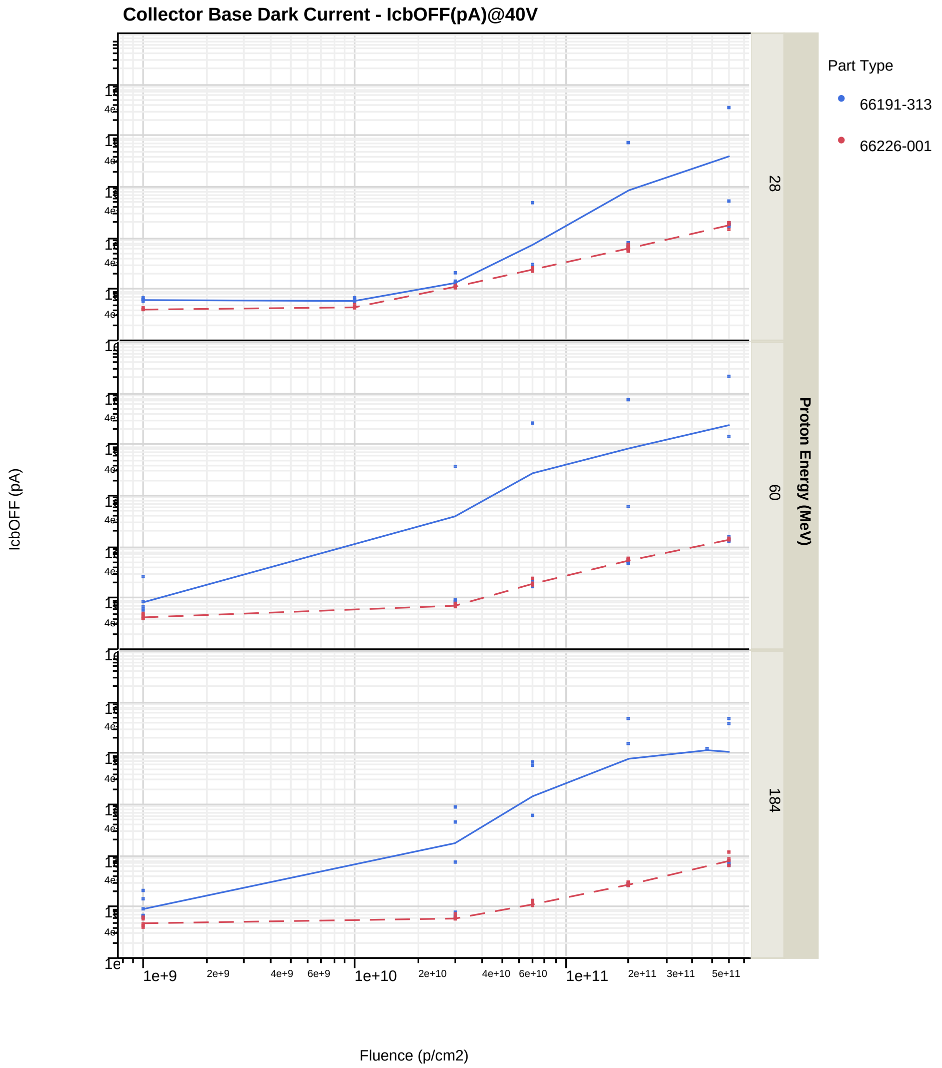

Fig. 3: Collector-base dark current drift. The points represent the measured data, and the line shows the trend of the average for each part type.

			Fluence (p/cm2)						
			1e+9	1e+10	3e+10	7e+10	2e+11	4.7e+11	6e+11
			y	y	y	y	y	y	y
Part type	Proton Energy (MeV)	SN	Mean	Mean	Mean	Mean	Mean	Mean	Mean
66191-313	28	#01	64	64	137	283	764	.	5064
		#02	62	59	126	259	678	.	1881
		#03	60	55	111	234	593	.	1591
		#04	63	59	128	258	683	.	1730
		#05	63	56	116	244	592	.	1623
		#06	64	66	206	4626	71830	.	341000
		#07	60	58	125	247	634	.	1549
		#08	59	58	127	257	678	.	1761
		#09	56	54	114	233	601	.	1674
	60	#10	58	.	83	209	5824	.	135400
		#11	63	.	80	181	508	.	1298
		#12	57	.	79	162	467	.	1188
		#13	58	.	80	175	525	.	1307
		#15	56	.	77	176	488	.	1270
		#16	57	.	76	175	495	.	1265
		#17	252	.	34780	245300	744300	.	2015000
		#18	62	.	85	190	542	.	1543
		#28	80	.	91	181	497	.	1184
	184	#19	62	.	.	121	273	.	674
		#20	65	.	66	114	261	.	608
		#21	67	.	73	125	280	.	666
		#22	59	.	62	113	257	.	626
		#23	205	.	8441	65480	476100	.	466300
		#24	90	.	726	5824	.	114800	.
		#25	64	.	74	123	269	.	708
		#26	140	.	4533	58210	148200	.	381000
		#27	64	.	66	118	262	.	618
66226-001	28	#01	42	45	112	247	667	.	1969
		#02	40	48	119	261	704	.	1839
		#03	38	42	108	234	577	.	1771
		#04	40	46	117	249	629	.	1868
		#05	41	42	102	214	536	.	1422
		#06	40	43	111	249	650	.	1847
	60	#07	39	.	70	183	556	.	1434
		#08	45	.	73	180	549	.	1350
		#09	37	.	67	230	525	.	1361
		#10	43	.	68	170	508	.	1345
		#11	47	.	76	181	546	.	1334
		#12	39	.	69	193	560	.	1459
	184	#13	44	.	58	115	289	.	752
		#14	45	.	55	103	250	.	625
		#15	56	.	61	106	241	.	642
		#16	59	.	70	126	291	.	1134
		#17	40	.	55	107	277	.	821
		#18	43	.	56	113	283	.	795

Table 6: Collector-base dark current at increasing fluence for each tested device.

4.2.2 Collector Emitter dark current drifts

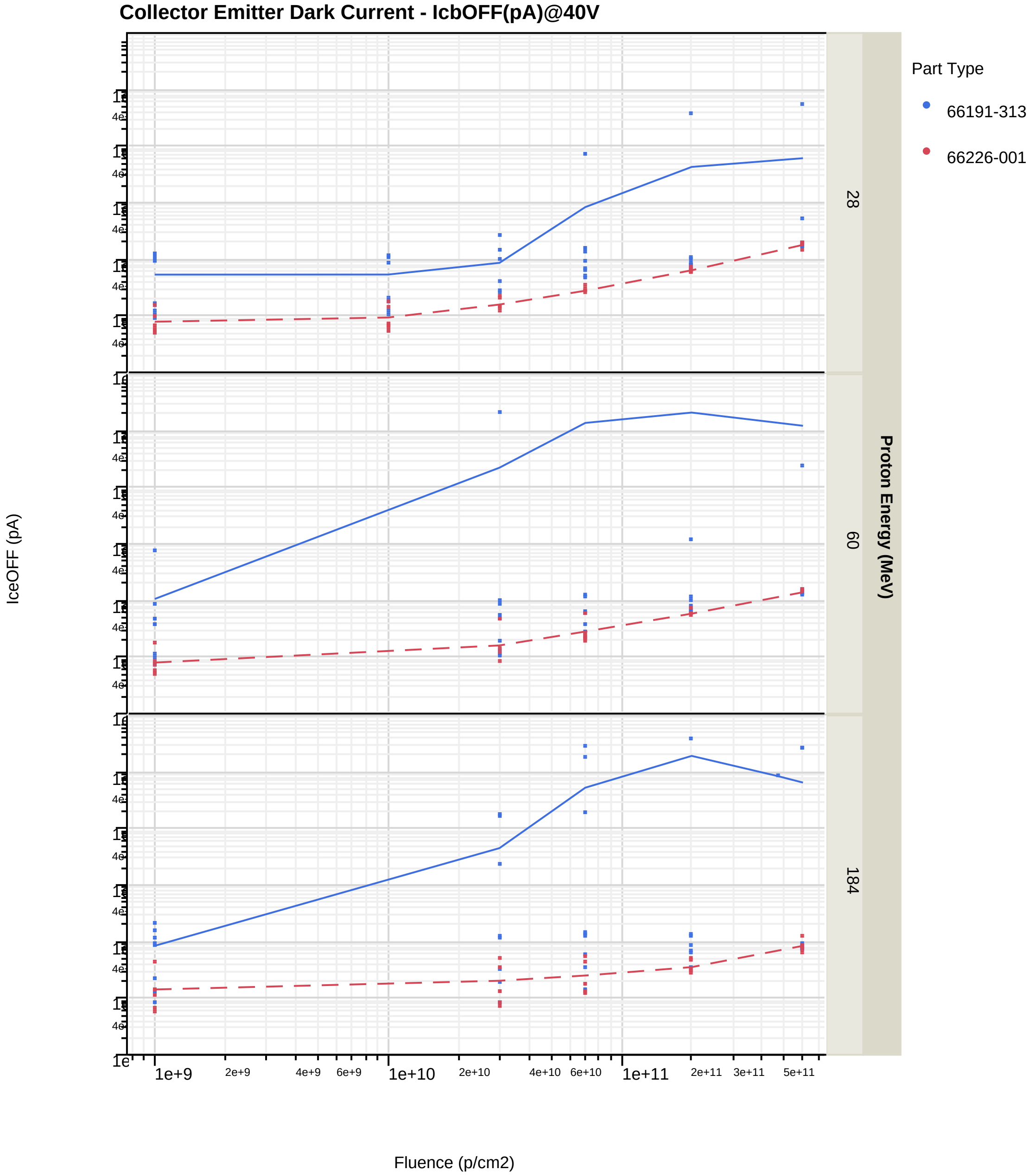

Fig. 4: Collector-emitter dark current at increasing fluence for each tested device. The points represent the measured data, and the line shows the trend of the average for each part type.

			Fluence (p/cm2)						
			1e+9	1e+10	3e+10	7e+10	2e+11	4.7e+11	6e+11
			y	y	y	y	y	y	y
Part type	Proton Energy (MeV)	SN	Mean	Mean	Mean	Mean	Mean	Mean	Mean
66191-313	28	#01	1044	1073	1343	1327	1044	.	5078
		#02	164	195	386	608	827	.	1905
		#03	154	177	385	651	791	.	1610
		#04	1222	1119	1372	1514	985	.	1749
		#05	116	122	270	465	682	.	1653
		#06	1012	1103	2557	68780	379500	.	533300
		#07	918	821	950	879	756	.	1576
		#08	89	103	245	501	850	.	1782
		#09	100	119	265	497	731	.	1690
	60	#10	70	.	104	270	12050	.	238800
		#11	107	.	183	379	786	.	1344
		#12	77	.	130	264	656	.	1225
		#13	466	.	860	1133	1130	.	1346
		#15	372	.	476	566	678	.	1294
		#16	812	.	1002	1236	978	.	1299
		#17	7221	.	1999000	12380000	18870000	.	10780000
		#18	357	.	530	629	760	.	1584
		#28	95	.	109	215	605	.	1213
	184	#19	884	.	.	1313	1229	.	837
		#20	81	.	83	142	354	.	712
		#21	1100	.	1237	1409	1322	.	852
		#22	216	.	325	579	863	.	799
		#23	815	.	176000	1823000	11500000	.	2662000
		#24	1503	.	22270	189400	.	841300	.
		#25	842	.	1152	1241	660	.	887
		#26	2039	.	158900	2729000	3880000	.	2526000
		#27	126	.	185	348	620	.	745
66226-001	28	#01	64	72	135	266	673	.	1983
		#02	153	171	220	335	723	.	1844
		#03	53	61	131	252	581	.	1793
		#04	48	51	118	251	630	.	1881
		#05	97	138	202	287	560	.	1431
		#06	58	67	144	275	663	.	1853
	60	#07	69	.	134	242	586	.	1448
		#08	56	.	85	186	559	.	1354
		#09	49	.	84	262	535	.	1371
		#10	53	.	85	197	530	.	1368
		#11	83	.	117	210	565	.	1343
		#12	169	.	457	595	731	.	1501
	184	#13	55	.	69	122	294	.	759
		#14	65	.	80	128	264	.	638
		#15	429	.	514	522	453	.	698
		#16	109	.	124	179	325	.	1258
		#17	56	.	81	130	292	.	849
		#18	143	.	354	430	500	.	861

Table 7: Collector-emitter dark current (Vce=40V) at increasing fluence for each tested device.

4.2.3 Collector Emitter dark current drifts

Manufacturer specification: $IceOFF_{MAX}$ = 100 nA

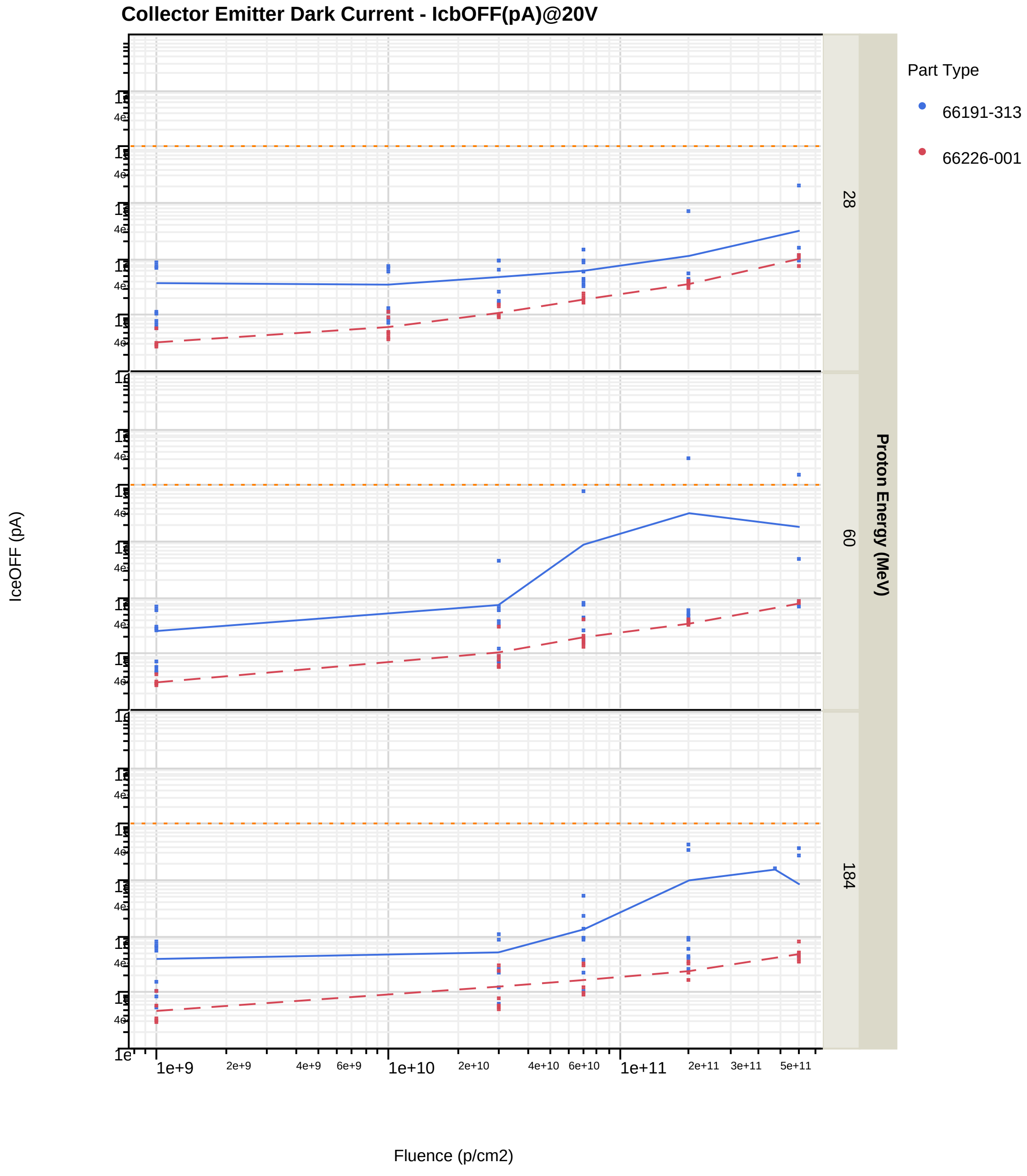

Fig. 5: Collector-emitter dark current drift. The points represent the measured data, and the line shows the trend of the average for each part type.

			Fluence (p/cm2)						
			1e+9	1e+10	3e+10	7e+10	2e+11	4.7e+11	6e+11
			y	y	y	y	y	y	y
Part type	**Proton Energy (MeV)**	**SN**	**Mean**	**Mean**	**Mean**	**Mean**	**Mean**	**Mean**	**Mean**
66191-313	28	#01	701	694	864	825	517	.	1521
		#02	107	126	247	396	432	.	1121
		#03	99	110	241	418	401	.	930
		#04	866	726	885	939	500	.	1086
		#05	77	81	172	311	358	.	972
		#06	717	709	919	1403	6820	.	20070
		#07	654	556	633	595	384	.	974
		#08	58	68	161	332	443	.	1097
		#09	67	78	171	328	377	.	955
	60	#10	45	.	70	149	466	.	4706
		#11	73	.	120	248	393	.	702
		#12	50	.	91	175	364	.	676
		#13	304	.	560	729	561	.	703
		#15	262	.	320	382	354	.	685
		#16	571	.	657	807	485	.	683
		#17	679	.	4408	76230	284100	.	153900
		#18	251	.	355	416	408	.	870
		#28	58	.	72	145	343	.	671
	184	#19	615	.	.	879	835	.	441
		#20	53	.	59	99	245	.	397
		#21	787	.	835	932	892	.	409
		#22	144	.	211	375	571	.	427
		#23	100	.	262	1291	43070	.	27550
		#24	652	.	1031	2149	.	15450	.
		#25	604	.	808	843	438	.	467
		#26	521	.	812	5144	32970	.	36990
		#27	83	.	122	225	405	.	411
66226-001	28	#01	31	48	93	188	387	.	1116
		#02	55	113	149	235	403	.	1103
		#03	27	39	92	180	334	.	1017
		#04	27	36	86	185	354	.	1040
		#05	30	86	138	156	290	.	749
		#06	28	45	99	194	384	.	1045
	60	#07	29	.	90	171	331	.	805
		#08	30	.	57	129	314	.	754
		#09	27	.	60	202	304	.	752
		#10	28	.	54	133	374	.	828
		#11	42	.	77	146	340	.	755
		#12	31	.	298	403	402	.	838
	184	#13	30	.	49	86	210	.	428
		#14	33	.	54	89	157	.	341
		#15	101	.	295	328	308	.	360
		#16	57	.	78	119	216	.	778
		#17	28	.	56	92	213	.	507
		#18	32	.	230	285	338	.	491

Table 8: Collector-emitter dark current (Vce=20V) at increasing fluence for each tested device.

4.3 Overall optocoupler performances

Two parameters were observed to characterize the overall optocouplers performances: the Collector Emitter Saturation Voltage and the CTR.

The VceSAT initial measurement of DUT#28 of 66191-313 was out of specification (0.432V instead of the limit of 0.3V). All the tested devices show an increasing VceSAT with increasing proton fluence, and several devices from both part types experience a drift of VceSAT to values higher than manufacturer specification, and at the last irradiation step the collector-emitter saturation voltage was over the compliance of 40 V set for the measurement (Table 9).

The CTR characterises the static efficiency of an the optocoupler, it is defined by the ratio of the photocurrent I_c corresponding to the LED current I_F:

$$CTR = \frac{I_c}{I_f}$$

The pre-irradiation CTR characteristic is reported in Par. 4.3.2. Different CTR performances and a different part to part uniformity can be observed on the two part types.
For comparison purposes the analyses in Par 4.3.3 and Par.4.3.4 refer to the same bias condition (CTR @ I_{LED}=10mA and V_{CE}=1V) of the manufacturer datasheet. At this measuring point the manufacturer specification indicates a minimum rated CTR of 1 .

Par. 4.3.3 contains the data of CTR degradation from proton irradiation, Par. 4.3.4 the normalized CTR showing the relative degradation from the initial measurements.

4.3.1 Collector Emitter Saturation Voltage Drift

Manufacturer specification: VceSAT$_{MAX}$ < 0.3V

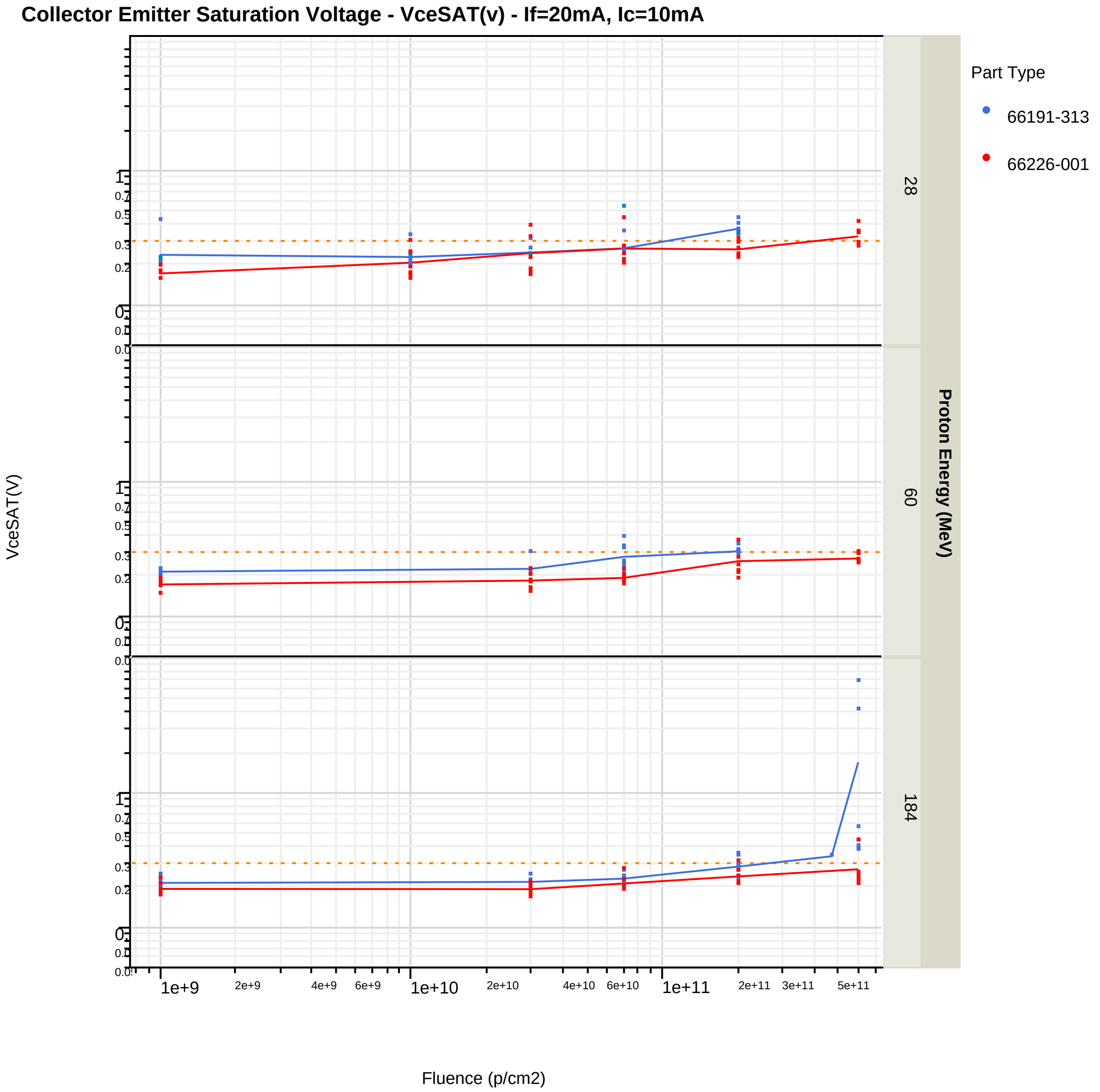

Fig. 6: Collector Emitter Saturation Voltage drift. The points represent the measured data, and the line shows the trend of the average for each part type. The orange dashed line indicates the manufacturer specification limit.

Part type	Proton Energy (MeV)	SN	Fluence (p/cm2) 1e+9	1e+10	3e+10	7e+10	2e+11	4.7e+11	6e+11
			y	y	y	y	y	y	y
			Mean	Mean	Mean	Mean	Mean	Mean	Mean
66191-313	28	#01	0.4327	0.3322	0.2392	0.271	0.4394	.	> 40
		#02	0.2133	0.2071	0.259	0.3519	0.3435	.	> 40
		#03	0.2056	0.2014	0.2331	0.2431	0.3342	.	> 40
		#04	0.2217	0.2358	0.2408	0.5428	0.3416	.	> 40
		#05	0.1975	0.2	0.2212	0.2411	0.3682	.	> 40
		#06	0.2176	0.2179	0.233	0.2565	0.3564	.	> 40
		#07	0.2246	0.2384	0.2367	0.2496	0.338	.	> 40
		#08	0.1957	0.22	0.3125	0.2414	0.3683	.	> 40
		#09	0.196	0.1958	0.2257	0.2491	0.3973	.	> 40
	60	#10	0.199	.	0.2065	0.3923	0.3354	.	> 40
		#11	0.2243	.	0.2234	0.2572	0.2972	.	> 40
		#12	0.2109	.	0.2024	0.2178	0.3135	.	> 40
		#13	0.2152	.	0.2178	0.243	0.2966	.	> 40
		#15	0.2047	.	0.2142	0.3272	0.2867	.	> 40
		#16	0.2214	.	0.2226	0.3201	0.2898	.	> 40
		#17	0.2148	.	0.2128	0.2385	0.2946	.	> 40
		#18	0.2153	.	0.3017	0.2414	0.3078	.	> 40
		#28	0.2152	.	0.214	0.237	0.3017	.	> 40
	184	#19	0.2441	.	.	0.2351	0.3355	.	4.154
		#20	0.211	.	0.2461	0.2311	0.2849	.	6.701
		#21	0.2429	.	0.2241	0.2347	0.2611	.	0.4465
		#22	0.2149	.	0.2248	0.2303	0.265	.	0.552
		#23	0.1857	.	0.1951	0.2068	0.2329	.	0.4398
		#24	0.2054	.	0.2129	0.2234	.	0.3362	.
		#25	0.2133	.	0.2178	0.2588	0.2404	.	0.4058
		#26	0.1992	.	0.2112	0.2224	0.2771	.	0.3804
		#27	0.2009	.	0.2024	0.2205	0.3568	.	0.389
66226-001	28	#01	0.1711	0.1921	0.3845	0.2714	0.3038	.	0.4168
		#02	0.1538	0.1571	0.3177	0.2147	0.2924	.	0.2935
		#03	0.1714	0.1647	0.1755	0.2102	0.2249	.	0.2703
		#04	0.178	0.1744	0.1833	0.1998	0.2387	.	0.3475
		#05	0.1965	0.2486	0.2265	0.4382	0.2314	.	0.3383
		#06	0.1551	0.2976	0.1662	0.2377	0.2593	.	0.2701
	60	#07	0.1855	.	0.1858	0.204	0.2153	.	0.2981
		#08	0.1883	.	0.1791	0.2211	0.2741	.	0.2559
		#09	0.1793	.	0.1995	0.1849	0.2085	.	0.2608
		#10	0.1677	.	0.1619	0.1976	0.1898	.	0.2857
		#11	0.1439	.	0.1498	0.1815	0.3666	.	0.2421
		#12	0.1776	.	0.226	0.1743	0.2379	.	0.2926
	184	#13	0.2095	.	0.1987	0.2006	0.2154	.	0.2532
		#14	0.1786	.	0.1887	0.1869	0.2592	.	0.2377
		#15	0.2281	.	0.2145	0.2201	0.2342	.	0.4453
		#16	0.1781	.	0.1805	0.1887	0.2067	.	0.2266
		#17	0.1727	.	0.1664	0.202	0.3064	.	0.2116
		#18	0.1867	.	0.1993	0.2672	0.2065	.	0.2398

Table 9: Collector emitter saturation voltage at increasing fluence for each tested device

4.3.2 Initial CTR measurement

The initial CTR characteristic of each DUT, is measured on a sweep of forward current (If=0.1 to 40mA), with a fix polarisation between collector and emitter (V_{CE}=1V).

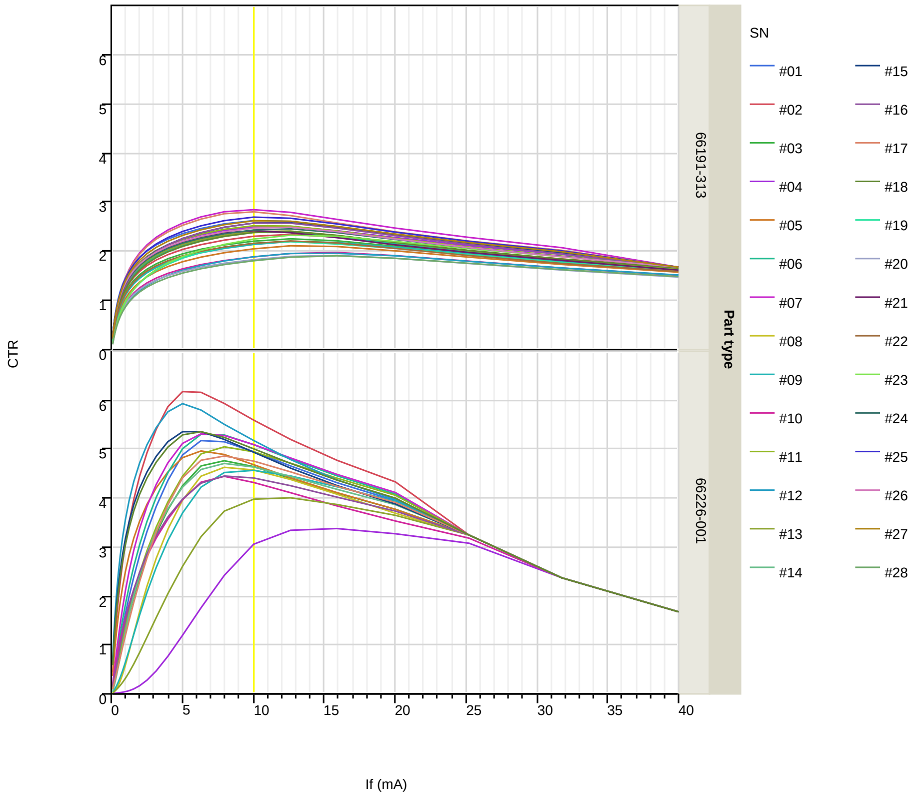

Fig. 7: CTR characteristic of each sample tested for each part type. The yellow line at If=10mA indicates the bias point selected for the subsequent CTR data analysis.

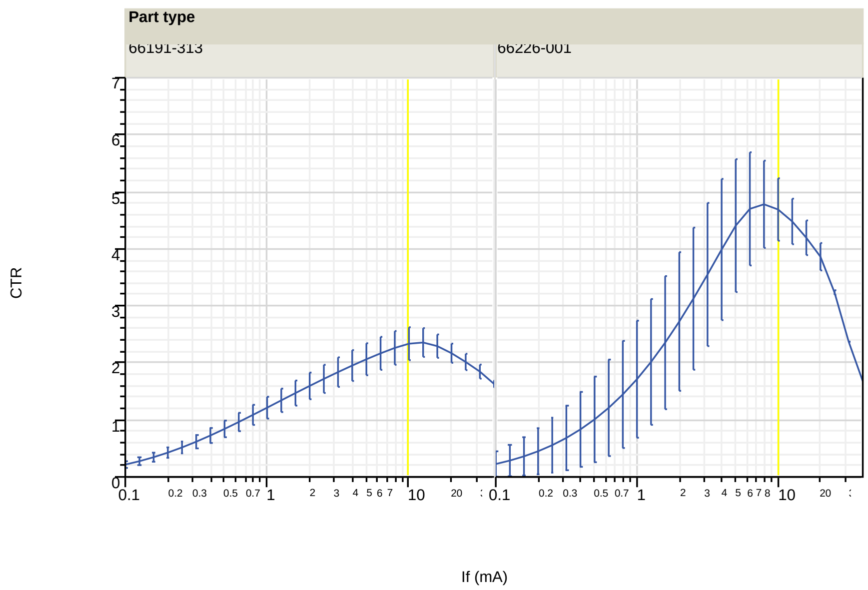

Fig. 8: Average CTR for the two part types, the error bars show the standard deviation for each measurement point. The yellow line on If=10mA indicates the bias point selected for the subsequent CTR data analysis.

4.3.3 CTR drifts

Manufacturer specification: minimum of CTR=1 @ I_{LED}=10mA and V_{CE}=1V.

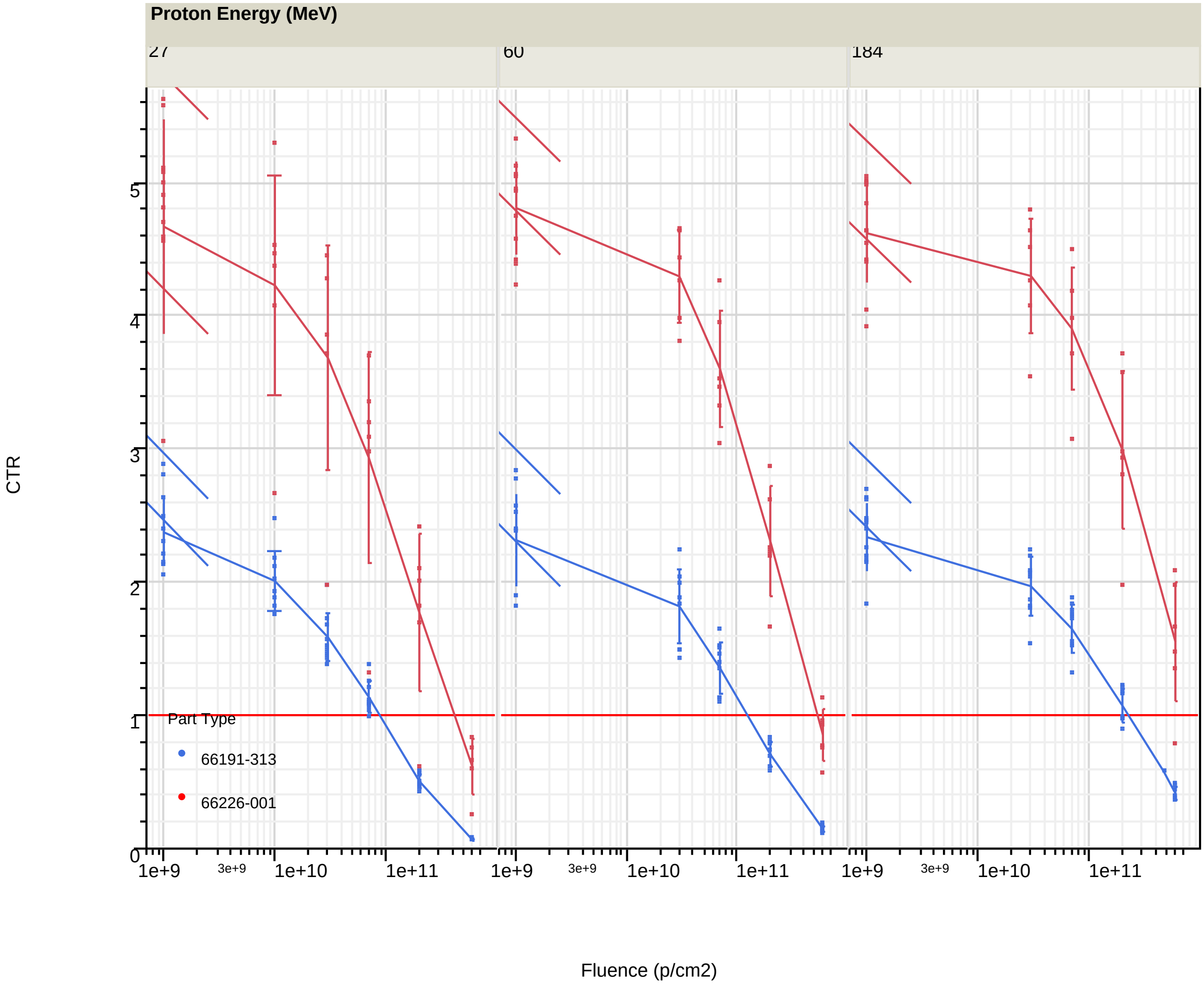

Fig. 9: Drift of average CTR_{DS} @ I_{LED}=10mA and V_{CE}=1V for 27, 60 and 184 MeV of proton beam energy. The points are the measured data, the lines show the trend of the average for each part type, the error bars the standard deviation.
The red line at CTR=1 is the value indicated in the manufacturer's datasheets as CTR minimum rating.

European Space Agency
Agence spatiale européenne

CTR□□@If=10mA, Vce=1V			Fluence (p/cm2)						
			1e+9	1e+10	3e+10	7e+10	2e+11	4.7e+11	6e+11
			y	y	y	y	y	y	y
Part type	Proton Energy (MeV)	SN	Mean	Mean	Mean	Mean	Mean	Mean	Mean
66191-313	28	#01	2.625	2.179	1.719	1.247	0.572	.	0.074
		#02	2.305	1.928	1.518	1.101	0.499	.	0.065
		#03	2.206	1.875	1.486	1.079	0.494	.	0.068
		#04	2.495	2.118	1.679	1.209	0.549	.	0.073
		#05	2.050	1.752	1.381	0.989	0.425	.	0.063
		#06	2.388	2.016	1.569	1.110	0.486	.	0.062
		#07	2.846	2.476	1.968	1.377	0.580	.	0.077
		#08	2.145	1.820	1.431	1.027	0.453	.	0.052
		#09	2.138	1.818	1.458	1.057	0.469	.	0.055
	60	#10	1.887	.	1.481	1.125	0.610	.	0.149
		#11	2.519	.	1.993	1.506	0.805	.	0.180
		#12	1.888	.	1.493	1.133	0.603	.	0.129
		#13	2.401	.	1.877	1.390	0.730	.	0.148
		#15	2.574	.	1.993	1.450	0.724	.	0.131
		#16	2.574	.	2.035	1.519	0.789	.	0.156
		#17	2.802	.	2.232	1.641	0.837	.	0.167
		#18	2.381	.	1.834	1.341	0.694	.	0.144
		#28	1.807	.	1.429	1.089	0.574	.	0.113
	184	#19	2.163	.	1.820	1.514	0.969	.	0.355
		#20	1.829	.	1.539	1.315	0.886	.	0.360
		#21	2.420	.	2.085	1.778	1.176	.	0.482
		#22	2.161	.	1.798	1.516	0.986	.	0.387
		#23	2.248	.	1.861	1.547	0.978	.	0.375
		#24	2.433	.	2.041	1.715	.	0.580	.
		#25	2.695	.	2.246	1.878	1.209	.	0.437
		#26	2.472	.	2.072	1.752	1.155	.	0.459
		#27	2.620	.	2.190	1.837	1.224	.	0.462
66226-001	28	#01	4.948	4.459	3.715	3.195	1.818	.	0.650
		#02	5.593	5.287	4.439	3.701	2.411	.	0.824
		#03	4.643	4.370	3.854	2.967	1.697	.	0.594
		#04	3.057	2.667	1.972	1.322	0.612	.	0.253
		#05	4.682	4.068	3.851	3.085	1.997	.	0.580
		#06	5.090	4.517	4.277	3.345	2.101	.	0.753
	60	#07	5.093	.	4.638	3.938	2.620	.	0.918
		#08	4.574	.	4.258	3.466	2.255	.	0.769
		#09	4.566	.	3.808	3.039	1.657	.	0.558
		#10	4.318	.	3.969	3.319	2.227	.	0.959
		#11	4.945	.	4.429	3.522	2.194	.	0.749
		#12	5.176	.	4.650	4.255	2.870	.	1.123
	184	#13	3.977	.	3.542	3.075	1.970	.	0.788
		#14	4.633	.	4.265	3.980	2.979	.	1.654
		#15	4.936	.	4.784	4.491	3.710	.	2.078
		#16	4.410	.	4.067	3.715	2.805	.	1.354
		#17	4.755	.	4.505	3.982	2.929	.	1.469
		#18	5.006	.	4.628	4.177	3.566	.	1.977

Table 10: CTR @ I_{LED}=10mA and V_{CE}=1V at increasing fluence for each tested device.

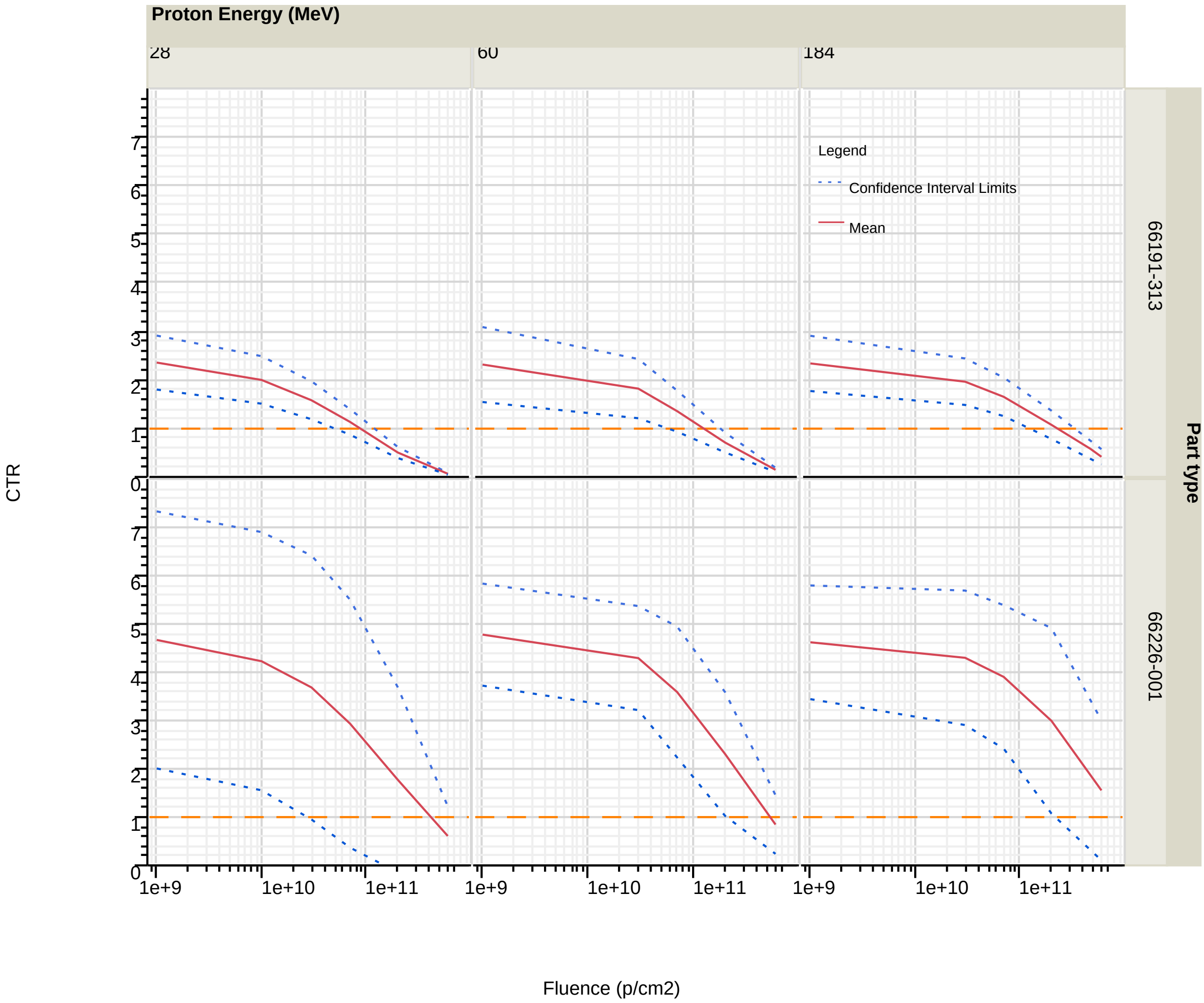

Fig. 10: The test data were statistically treated employing the one sided tolerance limit method. There is 90% probability with 90%confidence that the CTR(If=10mA,Vce=1V) will be within the confidence interval limits reported in the graph.

			Min Conf.Int.	Mean(y)	Max Conf.Int
Part type	Proton Energy (MeV)	Fluence (p/cm2)	Mean	Mean	Mean
66191-313	28	1e+9	1.7997152847	2.355	2.9108867516
		1e+10	1.508860127	1.998	2.4871558092
		3e+10	1.187757597	1.579	1.9700555946
		7e+10	0.8703572958	1.133	1.3951362854
		2e+11	0.3889814515	0.503	0.6171274462
		6e+11	0.0476210285	0.066	0.0834856559
	60	1e+9	1.5430199567	2.315	3.0867941204
		3e+10	1.2088597413	1.819	2.428369121
		7e+10	0.9318188161	1.355	1.778229878
		2e+11	0.5043468407	0.707	0.9105933983
		6e+11	0.1029924341	0.146	0.189991187
	184	1e+9	1.7690819213	2.338	2.9066595572
		3e+10	1.4827306935	1.961	2.4396420378
		7e+10	1.2528600111	1.65	2.0474941279
		2e+11	0.7812328763	1.073	1.3648079604
		4.7e+11	.	0.58	.
		6e+11	0.2574163238	0.415	0.571891445
66226-001	28	1e+9	2.0073775002	4.669	7.3301058996
		1e+10	1.5547905797	4.228	6.9010527138
		3e+10	0.9512150314	3.685	6.4179748757
		7e+10	0.3686704465	2.936	5.5028434978
		2e+11	-0.143429743	1.773	3.6886488665
		6e+11	-0.004243566	0.609	1.2220788914
	60	1e+9	3.7223265892	4.779	5.8349443272
		3e+10	3.2149984459	4.292	5.3693309034
		7e+10	2.2348243423	3.59	4.9447905315
		2e+11	1.023448531	2.304	3.5841211901
		6e+11	0.239010991	0.846	1.4527220767
	184	1e+9	3.4429067801	4.62	5.7966350526
		3e+10	2.9061557333	4.298	5.6907898178
		7e+10	2.4180428525	3.903	5.3887300558
		2e+11	1.0736308752	2.993	4.912756907
		6e+11	0.1047690886	1.553	3.0017382155

Table 11:
Mean CTR and 90% confidence of 90% probability intervals, plotted in Fig. 10.

4.3.4 Normalized CTR drifts

The normalized CTR is defined as the ratio of CTR measured at each tested fluence and the initial CTR.

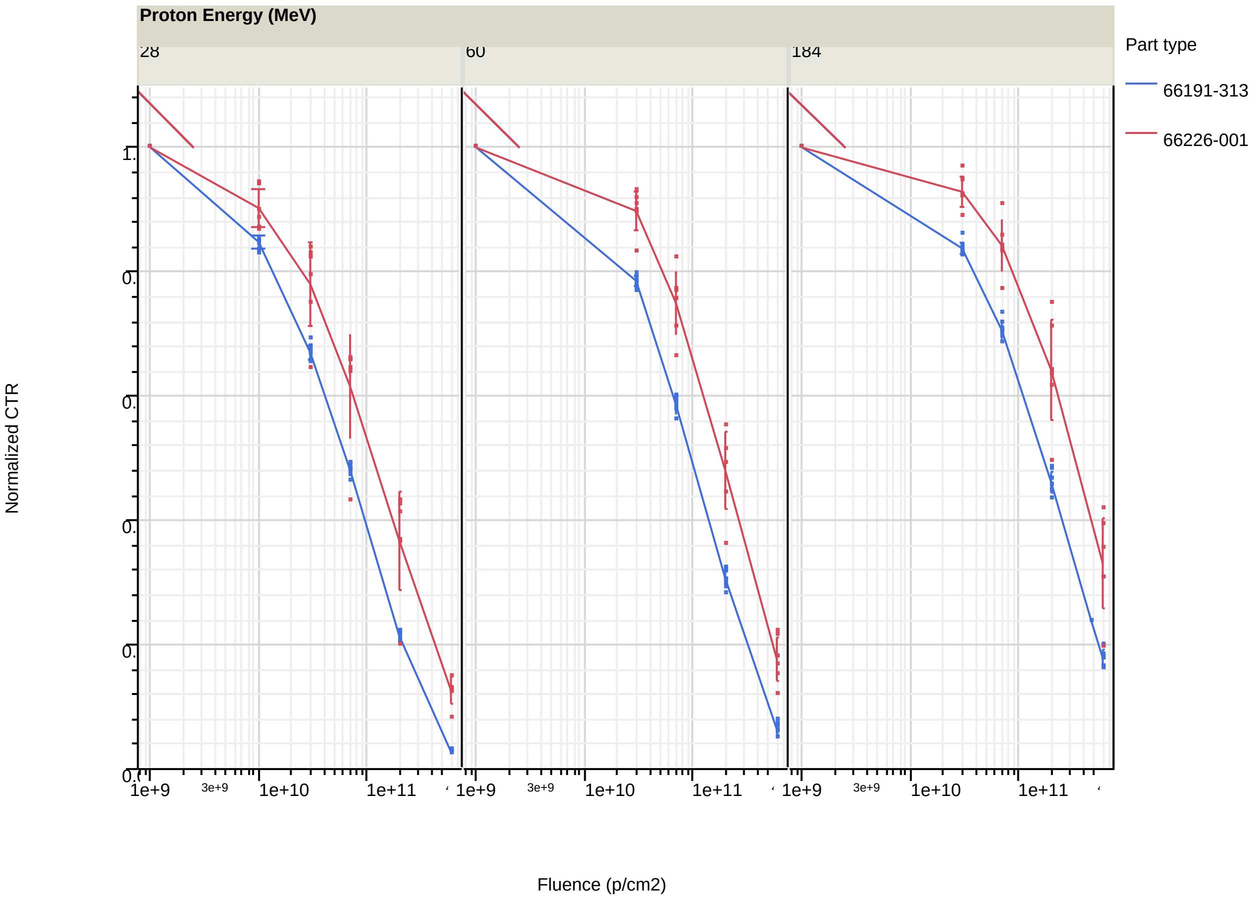

Fig. 11: Degradation of normalized CTR @ I_{LED}=10mA and V_{CE}=1V. The points are the measured data, the lines show the trend of the average for each part type, the error bars the standard deviation.

			Fluence (p/cm2)						
			1e+9	1e+10	3e+10	7e+10	2e+11	4.7e+11	6e+11
			ratio	ratio	ratio	ratio	ratio	ratio	ratio
Part type	Proton Energy (MeV)	SN	Sum	Sum	Sum	Sum	Sum	Sum	Sum
66191-313	28	#01	1.000	0.830	0.655	0.475	0.218	.	0.028
		#02	1.000	0.836	0.658	0.477	0.216	.	0.028
		#03	1.000	0.850	0.674	0.489	0.224	.	0.031
		#04	1.000	0.849	0.673	0.485	0.220	.	0.029
		#05	1.000	0.855	0.674	0.482	0.207	.	0.031
		#06	1.000	0.844	0.657	0.465	0.204	.	0.026
		#07	1.000	0.870	0.692	0.484	0.204	.	0.027
		#08	1.000	0.848	0.667	0.479	0.211	.	0.024
		#09	1.000	0.850	0.682	0.494	0.219	.	0.026
	60	#10	1.000	.	0.785	0.596	0.323	.	0.079
		#11	1.000	.	0.791	0.598	0.320	.	0.072
		#12	1.000	.	0.791	0.600	0.319	.	0.069
		#13	1.000	.	0.782	0.579	0.304	.	0.062
		#15	1.000	.	0.774	0.563	0.281	.	0.051
		#16	1.000	.	0.791	0.590	0.307	.	0.061
		#17	1.000	.	0.797	0.586	0.299	.	0.060
		#18	1.000	.	0.770	0.563	0.292	.	0.060
		#28	1.000	.	0.791	0.602	0.317	.	0.063
	184	#19	1.000	.	0.833	0.700	0.448	.	0.164
		#20	1.000	.	0.841	0.719	0.484	.	0.197
		#21	1.000	.	0.861	0.735	0.486	.	0.199
		#22	1.000	.	0.832	0.701	0.456	.	0.179
		#23	1.000	.	0.828	0.688	0.435	.	0.167
		#24	1.000	.	0.839	0.705	.	0.238	.
		#25	1.000	.	0.833	0.697	0.449	.	0.162
		#26	1.000	.	0.838	0.709	0.467	.	0.186
		#27	1.000	.	0.836	0.701	0.467	.	0.176
66226-001	28	#01	1.000	0.901	0.751	0.646	0.367	.	0.131
		#02	1.000	0.945	0.794	0.662	0.431	.	0.147
		#03	1.000	0.941	0.830	0.639	0.366	.	0.128
		#04	1.000	0.872	0.645	0.432	0.200	.	0.083
		#05	1.000	0.869	0.822	0.659	0.427	.	0.124
		#06	1.000	0.887	0.840	0.657	0.413	.	0.148
	60	#07	1.000	.	0.911	0.773	0.514	.	0.180
		#08	1.000	.	0.931	0.758	0.493	.	0.168
		#09	1.000	.	0.834	0.666	0.363	.	0.122
		#10	1.000	.	0.919	0.769	0.516	.	0.222
		#11	1.000	.	0.896	0.712	0.444	.	0.151
		#12	1.000	.	0.898	0.822	0.554	.	0.217
	184	#13	1.000	.	0.891	0.773	0.495	.	0.198
		#14	1.000	.	0.920	0.859	0.643	.	0.357
		#15	1.000	.	0.969	0.910	0.752	.	0.421
		#16	1.000	.	0.922	0.842	0.636	.	0.307
		#17	1.000	.	0.947	0.837	0.616	.	0.309
		#18	1.000	.	0.925	0.834	0.712	.	0.395

Table 12: Normalized CTR @ I_{LED}=10mA and V_{CE}=1V at increasing fluence for each DUT.

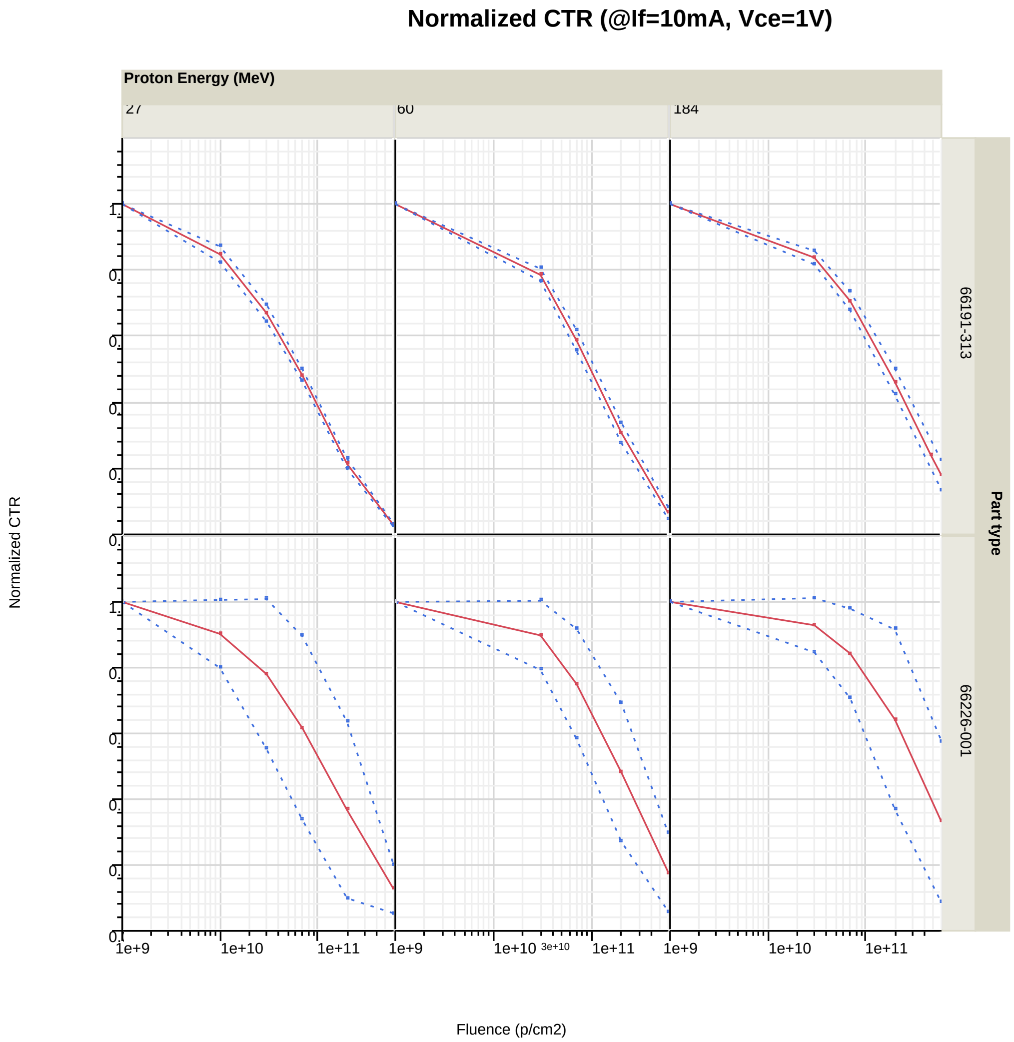

Fig. 12: Data were statistically treated employing the one sided tolerance limit method. There is 90% probability with 90% confidence that the CTR (If=10mA,Vce=1V) will be within the confidence interval limits reported in the graph.

CTR @ If =10mA, Vce=1V		y		ratio	
		Part type		Part type	
		66191-313	66226-001	66191-313	66226-001
Proton Energy (MeV)	Fluence (p/cm2)	Mean	Mean	Mean	Mean
28	1e+9	2.37	4.67	1	1
	1e+10	2.01	4.23	0.85	0.9
	3e+10	1.59	3.68	0.67	0.78
	7e+10	1.14	2.94	0.48	0.62
	2e+11	0.51	1.77	0.21	0.37
	6e+11	0.07	0.61	0.03	0.13
60	1e+9	2.31	4.81	1	1
	3e+10	1.82	4.3	0.79	0.9
	7e+10	1.36	3.6	0.59	0.75
	2e+11	0.71	2.31	0.31	0.48
	6e+11	0.15	0.85	0.06	0.18
184	1e+9	2.34	4.62	1	1
	3e+10	1.97	4.3	0.84	0.93
	7e+10	1.65	3.9	0.71	0.84
	2e+11	1.07	2.99	0.46	0.64
	4.7e+11	0.58	.	0.24	.
	6e+11	0.41	1.55	0.18	0.33

Table 13:
Summary of mean CTR and mean Normalized CTR degradation.
The mean is calculated on the tested samples for that irradiation condition.

5 CTR DEGRADATION AS A FUCTION OF DISPLACEMENT DAMAGE DOSE

As already stated, three proton energies were employed during the irradiation test campaign. The corresponding non-ionizing energy loss (NIEL) varies by a factor two from the lowest to the highest energy (28 to 184MeV respectively).

Since the optocouplers tested consist of a AlGaAs LED and photodiode while the output transistor is Si, NIEL for both materials have been considered. The results show better correlation with Si NIEL. It is therefore probable to assume that the Si output transistor is the main contributor to the device's DD sensitivity.

In the following analysis (Fig. 13 to Fig. 16) the test results for the three different energies employed have been plotted using the Displacement Damage Dose (DDD) deposited during irradiation. DDD was calculated as defined by

$$DDD = NIEL(E) \cdot \phi$$

where NIEL (MeV/ cm^2 g) is for protons in Si and ϕ is the proton fluence (proton/cm^2).
In addition to the DDD plots, the results have also been plotted as a function of 60MeV equivalent proton fluence. The 60MeV equivalent proton fluence was calculated by:

$$Equivalent\ 60\ MeV\ Fluence = \frac{NIEL\ (E)}{NIEL\ (60\ MeV)}\ \phi(E)$$

Proton Energy (MeV)	NIEL (Si) Mev*cm^2/g	Irradiation Fluence (p/cm2)			Normalized CTR degradation	
			DDD (Mev/g)	Equivalent 60MeV Fluence	66191	66226
28	0.00439	1.00E+09	4.39E+06	1.31E+09	1	1
		1.00E+10	4.39E+07	1.31E+10	0.85	0.9
		3.00E+10	1.32E+08	3.94E+10	0.67	0.78
		7.00E+10	3.07E+08	9.20E+10	0.48	0.62
		2.00E+11	8.78E+08	2.63E+11	0.21	0.37
		6.00E+11	2.63E+09	7.89E+11	0.03	0.13
60	0.00334	1.00E+09	3.34E+06	1.00E+09	1	1
		2.00E+10	6.68E+07	2.00E+10		
		3.00E+10	1.00E+08	3.00E+10	0.79	0.9
		7.00E+10	2.34E+08	7.00E+10	0.59	0.75
		2.00E+11	6.68E+08	2.00E+11	0.31	0.48
		6.00E+11	2.00E+09	6.00E+11	0.06	0.18
184	0.00187	1.00E+09	1.87E+06	5.60E+08	1	1
		3.00E+10	5.61E+07	1.68E+10	0.84	0.93
		7.00E+10	1.31E+08	3.92E+10	0.71	0.84
		2.00E+11	3.74E+08	1.12E+11	0.46	0.64
		4.70E+11	8.79E+08	2.63E+11	0.24	
		6.00E+11	1.12E+09	3.36E+11	0.18	0.33

Table 14: NIEL (Si) values of the three proton beam energies used. For each irradiation step the corresponding DDD (MeV/g) and the equivalent 60MeV proton fluence (p/cm^2) is reported.

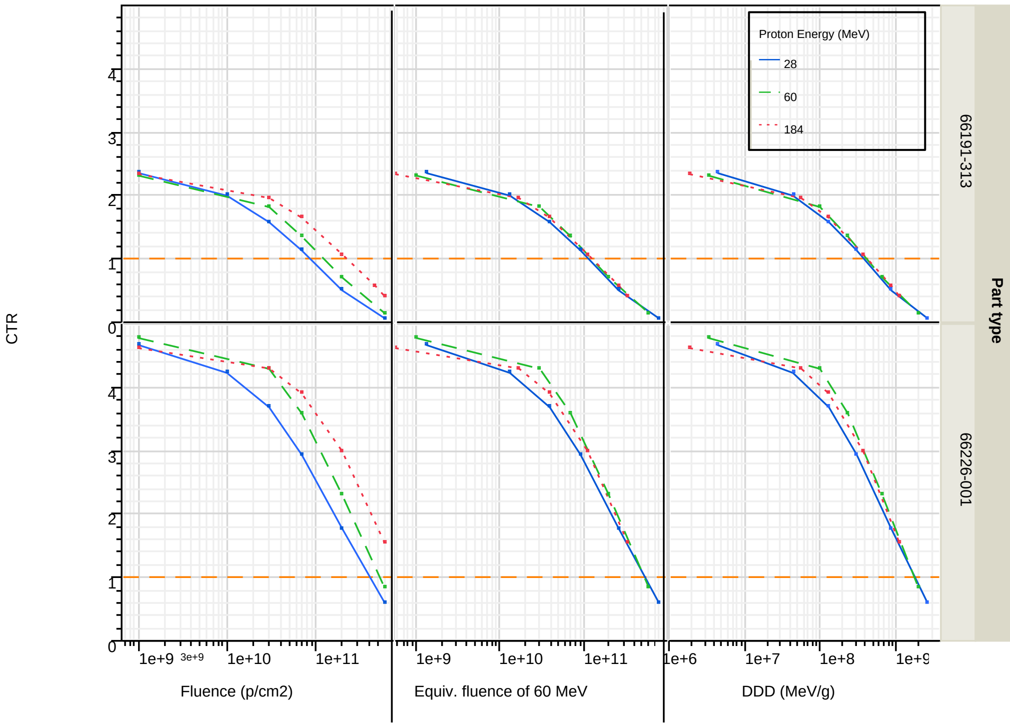

(a) (b) (c)

Fig. 13: CTR degradation for three different proton energies plotted as a function of received fluence (a), as a function of 60MeV equivalent proton fluence(b) as a function of displacement damage dose (c).

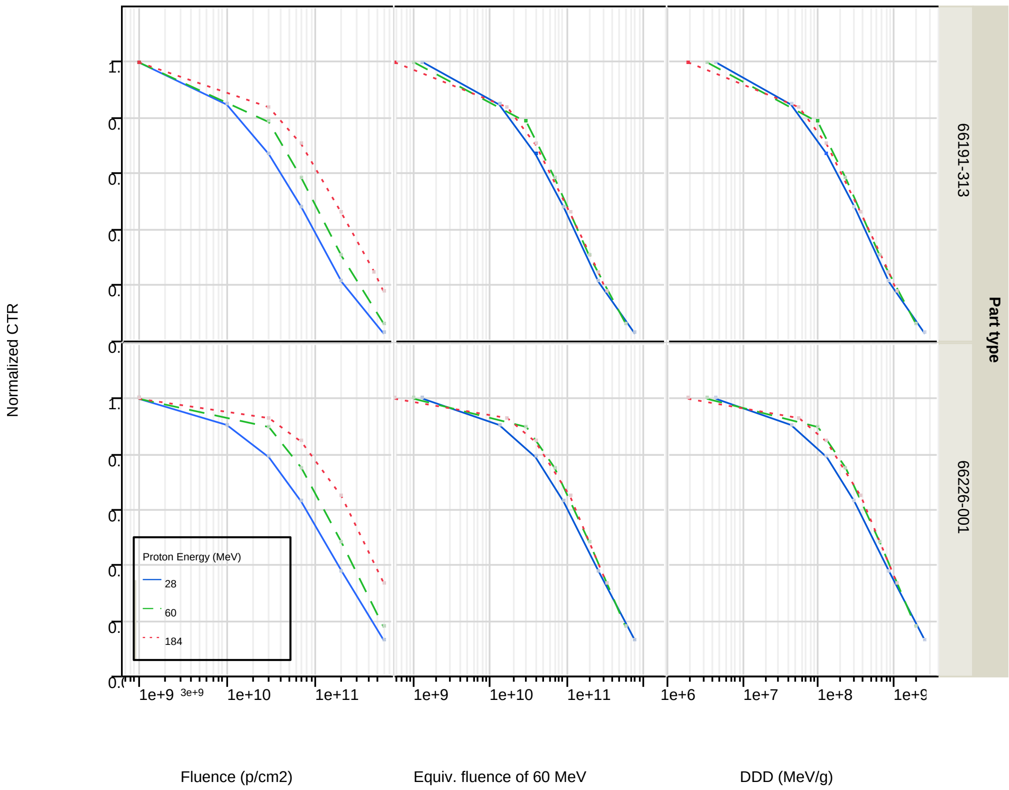

(a) (b) (c)

Fig. 14: Normalized CTR degradation for the three proton energies are plotted as a function of received fluence (a), as a function of 60MeV equivalent proton fluence (b) as a function of displacement damage dose (c).

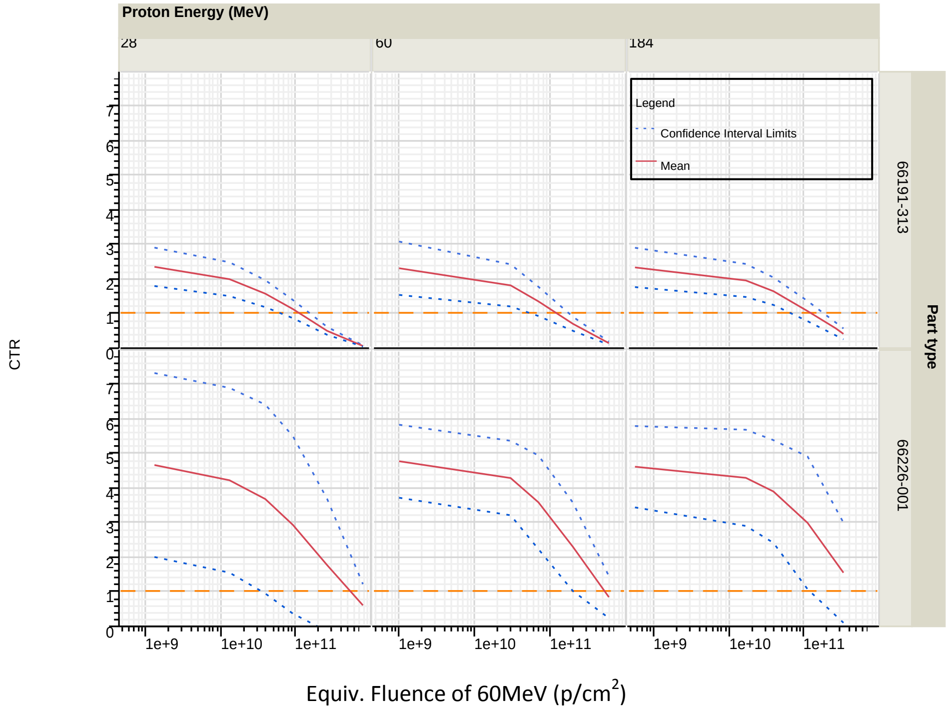

Fig. 15 CTR degradation as function of 60MeV equivalent proton fluence. Data were statistically treated employing the one sided tolerance limit method. There is 90% probability with 90% confidence that the CTR (If=10mA,Vce=1V) will be within the confidence interval limits reported in the graph.

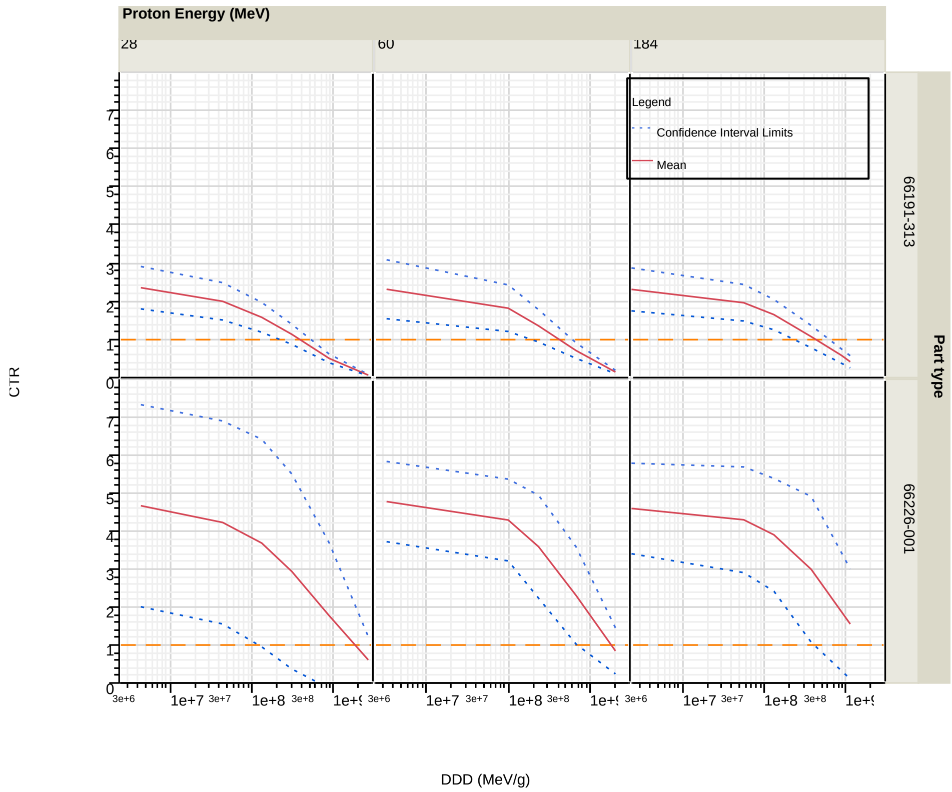

Fig. 16 CTR degradation as function of DDD. Data were statistically treated employing the one sided tolerance limit method. There is 90% probability with 90% confidence that the CTR (If=10mA,Vce=1V) will be within the confidence interval limits reported in the graph.

6 CONCLUSIONS

Considering the mean initial CTR on all tested samples (Fig. 8), 66226-001 has on average better performances than 66191-313, despite a larger part-to-part response non uniformity:
For the selected biasing point of CTR of If=10mA and Vce=1V on the initial characterisation:

-66191-313 has on average a CTR0=2.336 and a standard deviation of 0.289

-66226-001 has on average a CTR0=4.689 and a standard deviation of 0.547

The average CTR of the 66191-313 goes out of spec at a fluence between 8E+10 and 2E+11 protons/cm^2. However the average CTR of the 66226-001 device goes out of spec at a fluence greater than 4E+11 protons/cm^2 (Fig. 8) .

Notably, when the 90% probability, 90% confidence limits are taken into account the larger part-to-part non uniformity of 66226-001 (Fig. 10) impacts the fluence at which a failure is expected, and the degradation becomes comparable between the two part types:

- For 66191-313: 3E10 p/cm2 at 28 MeV, 2E11 p/cm2 at 60 MeV and 184 MeV,
- For 66226-001: 5E10 p/cm2 at 28 MeV, 6E10 p/cm2 at 60 MeV and 1E11 p/cm2 at 184 MeV.

From the decrease of the normalized CTR (Fig. 11) we can observe that the impact of proton irradiation is more relevant on CTR of 66191-313, but if the confidence interval limits are taken into account, the decrease of normalized CTR between the two part types are comparable (Fig. 12).

Please note that for project applications both DD and TID degradation shall be accounted for according to project RHA requirements.